CONVERSION OF KAPOK (*Ceiba pentandra* (L.) Gaertn.) HUSKS TO AN EFFICIENT ADSORBENT FOR BASIC BLUE 3 REMOVAL: BATCH ADSORPTION AND OPTIMIZATION STUDIES

JIN-YING TONG,[*] SIEW-TENG ONG[*,**] and SIE-TIONG HA[*,**]

[*]*Department of Chemical Science, Faculty of Science, Universiti Tunku Abdul Rahman, Jalan Universiti, Bandar Barat, 31900 Kampar, Perak, Malaysia*
[**]*Centre for Agriculture and Food Research, Universiti Tunku Abdul Rahman, Jalan Universiti, Bandar Barat, 31900 Kampar, Perak, Malaysia*
 Corresponding author: S.-T. Ong, ongst@utar.edu.my

Received July 24, 2025

Transforming wastes into usable materials is one of the routes to support sustainable development goals. In the current work, the feasibility of using Kapok husks as a promising adsorbent for the removal of Basic Blue 3 (BB3) was studied. Contact time, initial BB3 concentration, adsorbent dosage, agitation rate and pH were included in batch adsorption studies to examine their effects on the adsorption process. The equilibrium adsorption data was found to be best fitted to both Langmuir and BET isotherm model with an R^2 value of 0.9972 and maximum adsorption capacity of 197.1 mg/g. The adsorption of BB3 by Kapok husks was found to follow the pseudo-second order kinetic model, with R^2 close to unity. The functional groups present on Kapok husks were determined using Fourier transform infrared spectroscopy, and the surface morphology and topography were analyzed using scanning electron microscopy and atomic force microscopy, respectively. Plackett Burman design and Response Surface Methodology were used in the experimental design and optimization studies. The optimum conditions for maximum BB3 uptake were obtained as 180 minutes, 50 mg/L BB3 concentration, pH 10 and 0.03 g of Kapok husks. The system was able to achieve up to 98.20% adsorption under the optimum conditions.

Keywords: Kapok husks, Basic Blue 3, batch study, Plackett Burman design, Response Surface Methodology

INTRODUCTION

Over the past few decades, synthetic dyes have become widely accessible, driving rapid growth in industries such as the fashion and textiles industry. With over 100,000 commercially available dyes and an estimated global production of around 800,000 tons per year, the scale of dye usage is immense.[1] However, this widespread use has also contributed significant impacts to environmental pollution, particularly in water bodies. Among various sectors, textile industry stands out as one of the largest consumers of synthetic dyes and a key contributor to water pollution, primarily due to its highly water-dependent dyeing operations. It is estimated that nearly 15% of the dyes utilized in industries are discharged into the wastewater system, often without proper treatment.[2] This does not only degrade the water quality and harms aquatic ecosystems, but also presents potential health risks to humans as many dyes are toxic, carcinogenic and resistant to biodegradation.[3] Although synthetic dyes are favored for their vibrant colours, chemical stability and ease of applications, these same properties also contribute to their persistence and resistance to undergo natural breakdown in the environment.

Basic dyes tend to exhibit higher toxicity compared to other classes of dyes.[4] For instance, BB3, which is a classic example of basic dyes is toxic, mutagenic and carcinogenic.[5,6] It is known for its brilliant blue shade, and commonly used in textile industry for direct dyeing on acrylic carpet, acrylic blended fabric and silk, and dyeing wool. BB3 is frequently detected in the industrial wastewater, however, even at low concentrations, BB3 can cause serious ecological harm when discharged into aquatic environments.[7] It disrupts photosynthesis by limiting light penetration and

induces oxidative stress in aquatic organisms, as evidenced by the increase antioxidant enzyme activity in bivalves.[8] Apart from being aesthetically unpleasant in water bodies, structural damage to vital organs has also been observed, which highlights its cytotoxic and pathological effects.[8] Hence, contaminations due to dyes such as BB3 pose not only serious environmental problems, but also cause severe public health concerns.

Conventional wastewater treatment methods, including biological degradation, chemical oxidation, ion exchange and membrane filtration, often struggle to adequately remove dyes due to their inherent limitations.[9] In contrast, adsorption has gained significant attention as one of the most effective and versatile techniques for removal of pollutants due to its simplicity and operational flexibility. The potential for regeneration and reuse of adsorbents enhances the cost-effectiveness of adsorption by allowing multiple treatment cycles with minimal loss in efficiency.[10] Most importantly, it does not produce toxic or harmful by-products, thereby minimizing the risk of secondary environmental pollution.[11,12] Commercial activated carbon is widely recognized for its excellent adsorption capacity. However, its high production and regeneration costs along with environmental concerns limit its use. Therefore, many researchers have focused on low-cost adsorbents derived from industrial and agricultural waste as viable alternatives.[13-16]

Ceiba pentandra (L.) Gaertn. is a tropical tree and mostly found in southeast Asia. The tree and the cotton-like fibers harvested from its seed pods are commonly referred to as Kapok. This plant is highly versatile, with almost every part serving a purpose.[17] For example, the Kapok fibers are widely used as filling materials in pillows, mattresses, cushions and the oil extracted from the seeds serves in the production of fuel, soaps and lubricants.[17] However, the husks that make up a significant portion of the total weight of the Kapok fruit, remain largely underutilized as they are typically discarded as waste after harvesting. Kapok husks are also rich in organic compounds, which are key to adsorbing cationic pollutants. However, there is only limited research reported for adsorption of dyes using Kapok husks and a few examples are the removal of Rhodamine B[18] and Methylene Blue[19] dyes.

Therefore, given the limited research on the properties and applications of Kapok husks, this study aims to explore the potential of Kapok husks for BB3 removal through batch adsorption and optimization studies, with the goal of converting this underutilized waste into a valuable material.

EXPERIMENTAL

Adsorbent preparation

Kapok was collected and the husks were first separated from the attached Kapok fibers. Then, the Kapok husks were cut into smaller pieces. To remove the dirt particles and impurities, Kapok husks were thoroughly washed with tap water, followed by distilled water. After washing, they were subjected to drying in an oven at 60 °C for 24 hours to remove the moisture content. The dried Kapok husks were then ground into powder form using a grinder and screened through 425 µm sieve before storing them in a sealed bottle for future use.

Adsorbate preparation

BB3 was utilized as the adsorbate in this study. BB3, with a dye content of 25%, was obtained from Sigma Aldrich and used without any purification. It has a molecular formula of $C_{20}H_{26}ClN_3O$ with 359.89 g/mol of molecular weight. A standard dye solution of 1000 mg/L was prepared as stock solution and kept in the dark to prevent light degradation. Dilution was performed as needed to achieve the desired concentration for each experiment.

Batch studies

To determine the efficiency of Kapok husks in the removal of BB3, the effect of several factors, such as contact time, initial BB3 concentration, adsorbent dosage, agitation rate and pH, were investigated. Each run was carried out in duplicates, with the average results being reported. A control set without Kapok husks was also conducted to ensure that the removal of BB3 was due to the presence of Kapok husks itself rather than the wall of the centrifuge tube.

Batch adsorption of BB3 was performed in a centrifuge tube containing 20 mL of the BB3 solution to which Kapok husks were added. The mixture was then agitated on an orbital shaker. After the required contact time was reached, the mixtures were then centrifuged at 7000 rpm. The absorbance of the supernatant of the BB3 solution was analyzed using a UV-Vis spectrophotometer at the wavelength of 654 nm, where the maximum absorption takes place. Dilutions were performed when the measurement exceeded the linearity of the calibration curve. The percentage uptake of BB3 can be calculated referring to the following equation:

$$Percentage\ uptake\ of\ BB3 = \frac{C_o - C_t}{C_o}\ x\ 100\% \qquad (1)$$

where C_o = Initial BB3 concentration (mg/L), C_t = Concentration of BB3 at time, t (mg/L).

The effect of initial BB3 concentration was studied by adding 0.01 g of Kapok husks into 20 mL of three distinct concentrations of BB3 solutions, which were

50, 100 and 150 mg/L. The mixtures were agitated at 150 rpm. At predetermined time intervals, which were 1, 2, 3, 4, 5, 10, 15, 20, 25, 30, 45, 60, 120 and 180 minutes, the solutions were withdrawn from the orbital shaker and tested for their absorbance.

For the effect of adsorbent dosage, different amounts of Kapok husks ranging from 0.005 to 0.030 g, with 0.005 g intervals were added into 50 mg/L of BB3 solution. The mixtures were then subjected to agitation of 150 rpm for two hours to attain equilibrium. After measuring the absorbance of the supernatant solution, the final BB3 concentration was then calculated.

To study the effect of agitation rate towards the adsorption process, different agitation speeds, *i.e.* 50, 150 and 200 rpm, were used. The initial BB3 concentration and dosage of Kapok husks were kept constant at 50 mg/L and 0.01 g, respectively.

For the effect of pH, 0.01 g of Kapok husks was added into 50 mg/L of BB3 solution ranging from pH 2 to 10 and agitated for two hours at the speed of 150 rpm. The desired pH of BB3 were prepared by dropwise addition of 0.01, 0.05 and 0.10 M of NaOH and HCl solution.

In the determination of point of zero charge (pH_{pzc}) of Kapok husks, different concentrations of HCl and NaOH solutions (0.01, 0.05 and 0.10 M) were used to adjust 50 mg/L BB3 dye solution to different pH values ranging from 2 to 12. Each dye solution with the adjusted pH was then mixed with 0.01 g of Kapok husks and agitated at 150 rpm for 24 hours. The initial and final pH of dye solutions were compared after 24 hours. From the plot of ΔpH versus initial pH, pH_{pzc} can be obtained at the point where ΔpH equals zero, indicating the pH at which the surface of Kapok husks carries no net charge.

Sorption isotherms were studied by adjusting the dye solution concentrations from 10 to 100 mg/L. The results from adsorption kinetics and isotherm studies were subjected to linear regression analysis and the correlation coefficient, R^2 was calculated.

Characterization analyses

Fourier transform infrared spectroscopy

The presence of functional groups on the Kapok husks before and after the adsorption of BB3 was determined by FTIR, using a Spectrum RX1 by Perkin Elmer at the wavenumber range of 4000 to 400 cm^{-1}.

Scanning electron microscopy

The surface morphology of Kapok husks before and after adsorption of BB3 was analyzed using JEOL-JSM-6701 F SEM, which was operated at an acceleration voltage of 4.0 kV with 2000× magnification.

Atomic force microscopy

The surface topography of Kapok husks before and after adsorption of BB3 was analyzed using a Park XE-70 AFM, which is an instrument that scans the surface of a sample in a raster pattern to detect variations in surface structure at the atomic scale.

Optimization studies

Plackett-Burman design

The significancy of different variables towards the uptake of BB3 dye was studied and identified using the Plackett-Burman (PB) design. A total of five factors, including contact time, initial BB3 concentration, adsorbent dosage, agitation rate and pH, were investigated.

Response Surface Methodology

Using the significant factors identified through PB, further analysis and validation were carried out using RSM. RSM design yields a quadratic equation that can be used to model the relationship between the variables and the response, as well as to predict optimum conditions for maximum adsorption efficiency. Each experiment was conducted in duplicate and the response was determined by calculating the mean percentage of dye uptake. Design Expert Version 7.1.3 was employed for the entire experimental design and statistical analysis of the data.

RESULTS AND DISCUSSION

Batch studies

Effect of contact time and initial BB3 concentration

Figure 1 shows that prolonging the contact time leads to a better uptake of BB3. It was evident that a high adsorption capacity was achievable even at the initial stage of the adsorption process. A notable improvement in adsorption performance was observed initially, followed by a gradual slowdown, eventually reaching a steady and consistent trend over time. The rapid adsorption observed during the first 5 minutes was largely attributed to the abundant availability of active sites, facilitating the binding of BB3 molecules. It was suggested that a strong electrostatic attraction existed between the BB3 molecules and the Kapok husks. Over time, the adsorption rate slowed down as more and more BB3 molecules attached to the Kapok husks, leading to saturation of the active sites. At this stage, extending the contact time had a minimal impact, as few binding sites remained available. When all of the binding sites were fully saturated with the dye molecules, the uptake of BB3 stayed nearly constant as the contact time increased beyond the equilibrium.[20]

As observed from the figure, the trends of percentage uptake of dye over contact time were similar for all three concentrations of BB3. It could be seen that when the initial concentration of BB3 increased from 50 to 150 mg/L, the adsorption

capacity also increased. Increasing BB3 concentration resulted in more BB3 molecules being able to bind to the sites on the Kapok husks. This can be correlated to a stronger driving force to overcome the mass transfer resistance of BB3 towards the Kapok husks. A higher dye concentration could improve the interaction between the Kapok husks and BB3 which would lead to an elevated adsorption capacity.[21,22]

Effect of adsorbent dosage

Figure 2 presents the impact of various dosages of Kapok husks towards the uptake removal of BB3. From the figure, it was clear that when the dosage increased, the removal of BB3 also increased. This is because, increasing the amount of Kapok husks raised the number of available adsorption sites for BB3 to bind. By increasing the number of binding sites, the overall surface area and active sites available for adsorption became greater, thereby enhancing the likelihood for BB3 molecules to interact with Kapok husks.[23]

However, it was observed that there was no significant difference in the percentage uptake of BB3 when more than 0.01 g of Kapok husks was used. This was due to the fact that the dye molecules now became the limiting factor and saturation was reached.[24,25] Increasing the amount of adsorbent without increasing dye concentration lowered the adsorbate to adsorbent ratio. When all of the available BB3 dye molecules were adsorbed by the existing Kapok husks, increasing the dosage in this stage would not increase the uptake anymore, as there was no additional dye molecules for binding.

Effect of agitation rate

Figure 3 shows the effect of different agitation rates (50, 150 and 200 rpm) at various contact time on the adsorption of BB3. In the initial stage of the adsorption process, it was observed that the uptake of BB3 increased with increasing agitation rate. This could be due to the decrease in the thickness of the boundary layer surrounding the adsorbent.[26] Additionally, higher agitation enhanced the diffusion of dye molecules from the bulk solution to the surface of adsorbent.[27] When greater agitation speed was applied, it improved the mixing of the solution, ensuring a more uniform distribution of BB3 molecules, which came into contact with Kapok husks more efficiently.

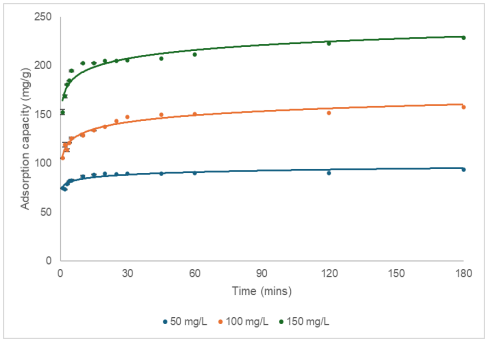

Figure 1: Effect of contact time and initial BB3 concentration towards adsorption

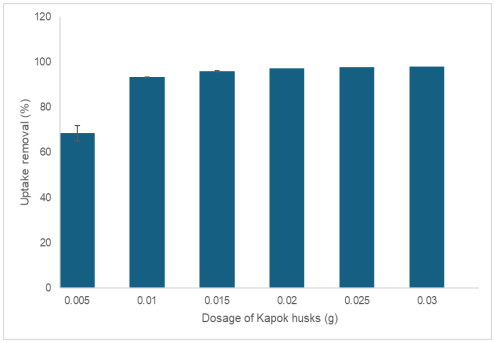

Figure 2: Effect of dosage of Kapok husks onto BB3 removal

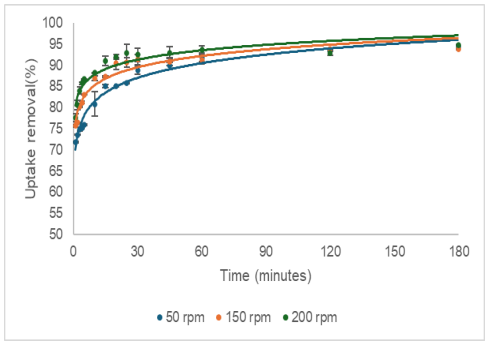

Figure 3: Effect of agitation rate on adsorption of BB3 by Kapok husks

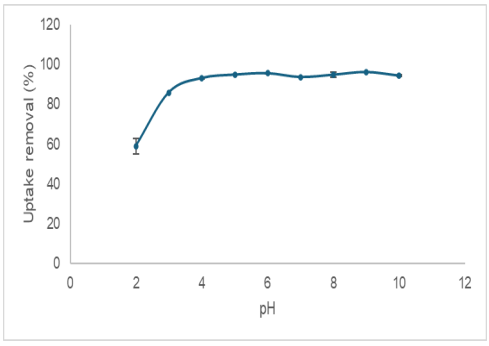

Figure 4: Effect of pH on the removal of BB3 using Kapok husks

Besides that, it could be seen that the process reached equilibrium faster when agitation rates of 150 and 200 rpm were used, as compared to 50 rpm.

Towards the end of the adsorption process, the three agitation rates converged to nearly the same uptake of BB3. This could be due to the fact that each system reached equilibrium and no further net adsorption could occur. Although higher agitation rate could accelerate the approach to equilibrium, the adsorption capacity of the adsorbent still remained unchanged in a given set of conditions. Essentially, once equilibrium was achieved, the adsorption capacity became limited by the maximum binding sites available rather than the rate of mass transfer, causing them to overlap in the end.

Effect of pH

The impact of pH ranging from pH 2 to 10 towards the ability of Kapok husks to adsorb BB3 was studied. Under extremely basic conditions, such as pH 11 and 12, BB3 demonstrated a decrease in its absorbance value and therefore these pH values were not included in this study.

Figure 4 shows that the adsorption system was able to achieve a high percentage uptake of BB3 in the range of pH 4 to 10. The adsorption performance is closely correlated to the point of zero charge, pH_{pzc}. The pH_{pzc} of Kapok husks was determined to be pH 6.3. Based on the figure, the lowest BB3 dye removal was observed at pH 2, where the percentage uptake was only 59%. As the pH increased from 2 to 4, a significant improvement in dye uptake was observed, with the percentage reaching as high as 93%. The dye uptake then remained nearly constant up to pH 10. The surface characteristics of Kapok husks have been found to be significantly impacted by the addition of acid. This is because at low pH conditions, the functional groups on the Kapok husks become protonated, resulting in a positively charged surface. This leads to electrostatic repulsion between the Kapok husks and BB3, which is a cationic dye, thereby reducing the adsorption efficiency.[28] Additionally, the low uptake could be attributed to the high H^+ ion concentration in acidic conditions, which competes BB3 dye molecules for the active sites. Dye sorption relies on the protonation and deprotonation of certain functional groups of the adsorbent. Hence, conversely when the pH was greater than the pH_{pzc}, a high dye uptake was expected. This was due to the presence of negatively charged surface on the Kapok husks, resulting from deprotonation, which attracts the positively charged BB3 dye through electrostatic interaction.[29]

Adsorption isotherm

Langmuir isotherm

The Langmuir adsorption isotherm model is built on several assumptions where adsorption is limited to a single molecular layer on the surface and each molecule attaches to a distinct, individual site. In addition, there are no interactions between adsorbed molecules at different sites, and the enthalpy of adsorption remains uniform across all sites, regardless of the surface coverage.[30]

The Langmuir isotherm is depicted as follows:

$$q_e = \frac{q_m K_L C_e}{1+K_L C_e} \quad (2)$$

Equation (2) could be linearized and the linear form is represented by:

$$\frac{C_e}{q_e} = \frac{1}{q_m K_L} + \frac{C_e}{q_m} \quad (3)$$

where C_e = concentration BB3 at equilibrium (mg/L), q_e = amount of BB3 adsorbed at equilibrium (mg/g), q_m = maximum adsorption capacity of Kapok husks (mg/g), K_L = Langmuir isotherm constant related to energy of Kapok husks (L/mg).

The Langmuir isotherm constant, K_L and the maximum adsorption capacity of Kapok husks were found to be 0.3091 L/mg and 196.1 mg/g, respectively. Compared to several previously reported adsorbents, the calculated q_m in this study is relatively high, which highlighted the potential of Kapok husks as an efficient and promising adsorbent for dye removal applications.[28,31,32] Besides, the linearized Langmuir plot (Fig. 5), the coefficient of determination, R^2 value of 0.9971 was obtained, indicating a strong fit and suggesting that monolayer adsorption occurred on a homogeneous surface.

Freundlich isotherm

The Freundlich isotherm describes multilayer adsorption on heterogeneous sites by assuming non-uniform affinities and heat distribution during adsorption. It is typically used for non-ideal adsorption, suggesting diverse types of binding sites with different free energies of adsorption acting simultaneously.[33]

The Freundlich isotherm model is defined as:

$$q_e = K_F C_e^{\frac{1}{n}} \quad (4)$$

By taking the logarithm on both sides for Equation (4), the linearized equation is expressed as:

$$\log q_e = \frac{\log C_e}{n} + \log K_F \quad (5)$$

where q_e = amount of BB3 adsorbed at equilibrium (mg/g), C_e = concentration of BB3 at equilibrium (mg/L), n = Freundlich constant for intensity, K_F = Freundlich isotherm constant for adsorption capacity.

The experimental data demonstrated a reasonable fitting of the data to the Freundlich isotherm model, with an R^2 value of 0.9699. Based on Equation (5), the slope and y-intercept resulted in a n value of 1.806 and K_F value of 41.50 mg/g, respectively. Since n falls between 1 and 10, the adsorption of BB3 is considered favourable, further demonstrating that the adsorption process is an effective approach for BB3 dye removal.

Brunauer-Emmett-Teller (BET) isotherm

The BET model is basically an extension of the Langmuir isotherm that considers the possibility of multilayer adsorption. It was built on the assumption that physisorption allows multilayers of adsorbate on the surface of the adsorbent. This model also assumes that each adsorption site work independently and the surface has uniformly distributed sites. Once a complete monolayer is formed, additional layers could build up successively. Also, it assumes that the energy of adsorption is the same at every site.[34]

The BET isotherm model is represented as:

$$q_e = \frac{K_B q_m C_e}{(C_S - C_e)[1 + (K_B - 1)\left(\frac{C_e}{C_S}\right)]} \quad (6)$$

In linear form, the equation is written as:

$$\frac{C_e}{(C_S - C_e)q_e} = \left(\frac{K_B - 1}{K_B q_m}\right)\left(\frac{C_e}{C_S}\right) + \frac{1}{K_B q_m} \quad (7)$$

where q_e = amount of BB3 adsorbed at equilibrium (mg/g), K_B = BET constant, which describes the energy involved in the adsorbate-adsorbent interaction, q_m = amount of BB3 in the formation of the complete monolayer (mg/g), C_e = concentration of BB3 at equilibrium (mg/L), C_s = BB3 concentration at saturation (mg/L).

According to Equation (7), a linear plot was constructed (Fig. 6). The values of K_B and q_m were determined to be 88125 and 197.1 mg/g, respectively, based on the slope and y-intercept. The BET plot yielded a R^2 value of 0.9972, indicating that this can be a suitable model to describe the adsorption behaviour. Table 1 shows the comparison of different isotherm parameters and R^2 values for the Langmuir, Freundlich and BET isotherm models.

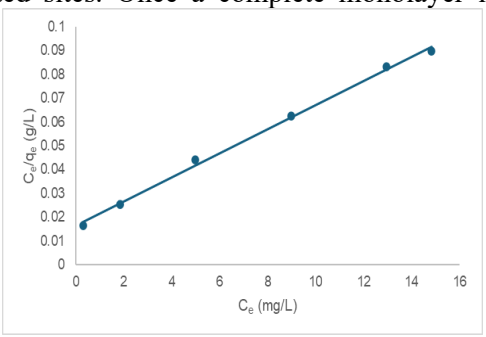

Figure 5: Langmuir isotherm plot for the adsorption of BB3 by Kapok husks

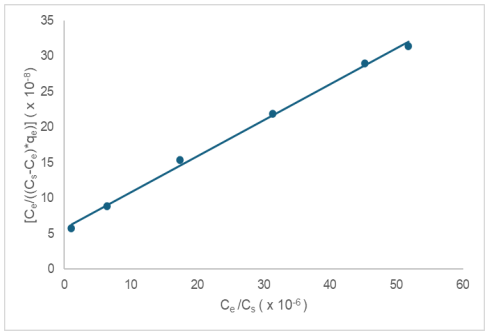

Figure 6: BET isotherm plot for the adsorption of BB3 by Kapok husks

Table 1
Isotherms parameters and R^2 values in BB3 adsorption by Kapok husks

Langmuir isotherm		Freundlich isotherm		BET isotherm	
q_m (mg/g)	196.1	n	1.806	q_m(mg/g)	197.1
K_L (L/mg)	0.3091	K_F	41.50	K_B	88125
R^2	0.9971	R^2	0.9699	R^2	0.9972

By comparing the R^2 value in Table 1, it can be seen that all isotherm models show very high R^2 value, which is close to unity. However, both Langmuir and BET isotherm models demonstrated higher correlation of determination compared to the Freundlich isotherm model. Hence, the findings suggested that the adsorption initially formed a single layer on a uniform surface with a finite number of sites before proceeding to the formation additional layers beyond the monolayer.

Adsorption kinetics

Pseudo-first order kinetic model

The Lagergren pseudo-first order kinetic model assumes that the adsorption rate is influenced by the concentration of the adsorbate and the availability of adsorption sites on the adsorbent. It also suggested that the process is controlled by physisorption, with diffusion of the adsorbate on the surface of adsorbent playing a key role.[35]

The pseudo-first order kinetic model can be represented as:

$$\frac{d_q}{d_t} = k_1(q_e - q_t) \quad (8)$$

After integrating and taking into consideration the boundary conditions, the final equation is:

$$\log(q_e - q_t) = \log q_e - \frac{k_1}{2.303} t \quad (9)$$

where q_e = amount of BB3 adsorbed at equilibrium (mg/g), q_t = amount of BB3 adsorbed at time t (mg/g), k_1 = pseudo-first order kinetics rate constant (min^{-1}), t = time (minutes).

By referring to Table 2, it was observed that the pseudo-first order model may not be adequately representing the studied concentration range. The R^2 values across the three data sets also clearly showed large deviation from unity. Additionally, the calculated equilibrium adsorption capacities deviated significantly from the experimental results. As a result, the model was considered inappropriate for representing the adsorption of BB3 onto Kapok husks.

Pseudo-second order kinetic model

Ho's pseudo-second order kinetic model assumes that chemisorption, involving valence forces through sharing or exchange of electrons is the rate determining step.[36] In this case, the rate of adsorption is proportional to the square of the number of unoccupied active sites on the adsorbent.

The pseudo-second order kinetics model is written as:

$$\frac{dq_t}{dt} = k_2(q_e - q_t)^2 \quad (10)$$

After applying the boundary conditions and integration, the final pseudo-second order model equation in linearized form is as follows:

$$\frac{t}{q_t} = \frac{1}{h} + \frac{t}{q_e} \quad (11)$$

$$h = k_2 q_e^2 \quad (12)$$

where q_t = amount of BB3 adsorbed at time t (mg/g), k_2 = pseudo-second order kinetics rate constant (g/mg min), q_e = amount of BB3 adsorbed at equilibrium (mg/g), h = initial adsorption rate (mg/g min).

Based on Equation (11), a plot of t/q_t against t displayed a linear trend (Fig. 7). For each concentration of dye, all the values were calculated and tabulated in Table 2. It was found that the pseudo-second order rate constant, k_2 decreased with increasing concentration of BB3. This was likely due to increase competition for active sites at higher concentration, whereas at lower concentration of BB3, less competition allowed for faster adsorption. According to the findings, the close match between the calculated and experimental q_e values, along with consistently high R^2 values nearing unity, indicated that the pseudo-second order kinetic model provides a more reliable fit for the data compared to the pseudo-first order model. This strong correlation suggested that the adsorption of BB3 onto Kapok husks is better explained by a chemisorption mechanism, where chemical bonding plays a key role in the interaction between the adsorbate and adsorbent. Apart from the electrostatic attraction, it is also believed that the hydroxyl groups present on the surface of Kapok husks played a role in hydrogen bonding with nitrogen atoms of BB3 dye molecules.

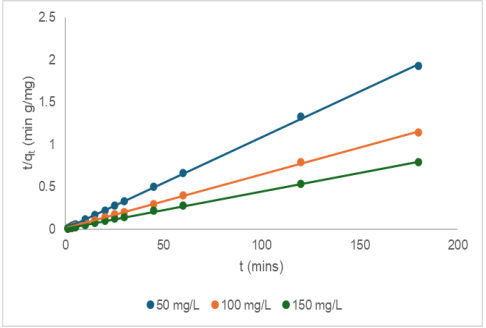

Figure 7: Pseudo-second order plot for the adsorption of BB3 by Kapok husks

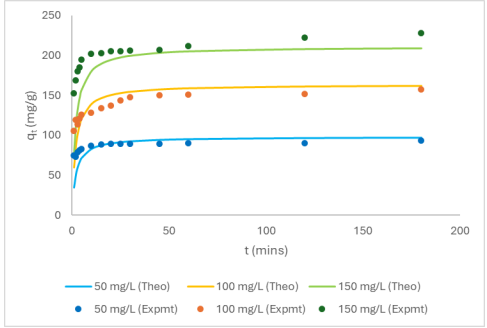

Figure 8: Theoretical model of BB3 adsorption onto Kapok husks

Table 2
Comparison between pseudo-first and second order kinetic model in terms of adsorption capacities, kinetic model parameters and correlation coefficients

Initial BB3 concentration (mg/L)	Pseudo-first order			Pseudo-second order				$q_{e,exp}$ (mg/g)
	$q_{e,cal}$ (mg/g)	k_1 (min^{-1})	R^2	$q_{e,cal}$ (mg/g)	k_2 ($x10^{-3}$ g/mg min)	h (mg/g·min)	R^2	
50	15.4597	0.0078	0.3264	96.1538	5.9429	54.9451	0.9967	93.5279
100	32.5987	0.0196	0.7443	156.2500	3.5310	86.2069	0.9995	157.5000
150	40.0405	0.0228	0.8329	222.2222	2.7740	136.9863	0.9996	228.3631

The theoretical model for BB3 could be expressed as follows:

$$q_t = \frac{C_o t}{(0.0028)(C_o) + 0.7812 + (0.002\ C_o + 0.4117)t} \quad (13)$$

From the literature, it has also been demonstrated that the pseudo-second order kinetic model can be used as an appropriate model to describe effectively the adsorption behaviour of dyes.[16,23,37,38]

Figure 8 presents a comparison between the experimental data and the theoretical model of BB3 adsorption. It was evident that the theoretically generated curves agreed well with the experimental data. Hence, this further supported the findings that the adsorption of BB3 by Kapok husks followed the pseudo-second order kinetic model.

Characterization analysis

FTIR studies

FTIR was used to identify the functional groups in Kapok husks involved in the adsorption of BB3. The spectra before and after adsorption are shown in Figure 9, with important peaks and their corresponding functional groups summarized in Table 3.

Kapok husks contain a high percentage of organic compounds, such as cellulose, hemicelluloses and lignin. According to the IR spectrum recorded before adsorption, a strong and broad absorption band was observed at 3405 cm^{-1}. This peak corresponds to the OH stretch in lignocellulosic materials, indicating phenolic compounds and alcohols from hemicelluloses, lignin and cellulose in the Kapok husks.[19] The band at 2923 cm^{-1} showed the occurrence of CH stretching vibration.[18] These two absorption bands were significant as they originated from the hydroxyl groups and numerous CH bonds, which are common structural features in the primary biomass components – cellulose, hemicelluloses and lignin. Beyond that, the spectrum showed a band at 1620 cm^{-1}, attributed to the presence of asymmetric stretching of the carboxyl group in glucuronic acid from hemicelluloses, as well as the stretching of conjugated carbonyl (C=O) groups present in lignin.[39-42] The band attributed to CH_2 symmetric bending and CH in-plane deformation coupled with aromatic ring stretching in lignin appeared around 1422 cm^{-1}.[43,44] The presence of CH_2 wagging and CO stretching vibration of substituted aromatic units were found at 1318 cm^{-1}, whereas the band around 1152-1061 cm^{-1} could be due to the elongation vibration of C-O bonds in ethers, phenols and alcohols.[42,45,46] The band appearing at 893 cm^{-1} may be due to the C-O-C stretching vibration at the β-(1→4)-glycosidic linkages in cellulose and hemicelluloses.[45,47]

After the adsorption of BB3, it was found that the functional groups in the spectrum showed minimal differences. Since dye removal primarily involves surface interactions during adsorption, the spectrum was expected to display only minor changes and appear quite similar.[48] The intensities of the peaks also reduced after adsorption. Similar observations have been reported in previous studies for adsorption.[49-51] After the adsorption of BB3, the peaks originally appearing at 2923, 1422, 1318 and 1061 cm^{-1} shifted to 2922, 1403, 1335 and 1067 cm^{-1}, respectively. More obvious peak shifting before and after adsorption is illustrated in Figure 9. The peak due to hydroxyl group was greatly shifted from 3405 to 3414 cm^{-1} and the intensity of the peak is also reduced after BB3 adsorption. This observation suggests the interaction between the negatively charged hydroxyl group of Kapok husk with the positively charged BB3 cation.[28] Other evidence suggesting the successful binding of BB3 dye onto the Kapok husk is the peak due to the C-N stretching of aromatic tertiary amine of BB3 dye, which can be observed at 1335 cm^{-1} in the Kapok husk spectrum after adsorption. This peak value falls within the range reported for BB3 dye.[52]

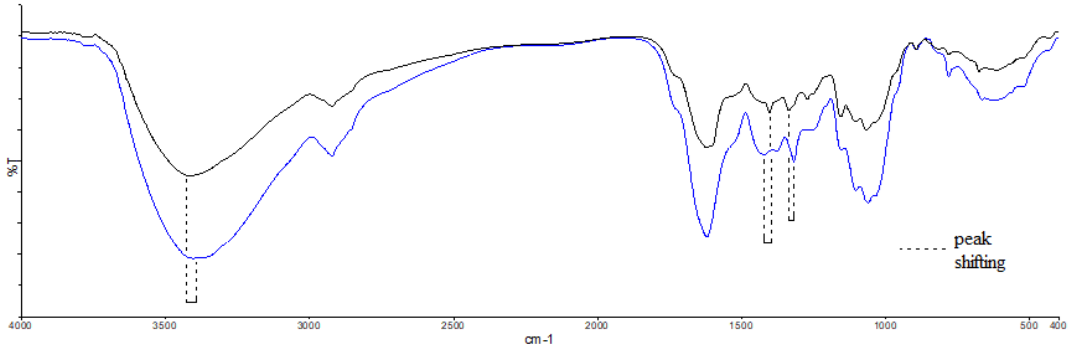

Figure 9: FTIR spectra of Kapok husks before (blue) and after (black) adsorption of BB3

Table 3
Comparison of FTIR peaks before and after adsorption of BB3

Wavenumber (cm^{-1})		Assignment
Before adsorption	After adsorption	
3405	3414	OH stretching
2923	2922	CH stretching
1620	1620	C=O stretching
1422	1403	CH_2 bending, CH deformation
1318	1335	CH_2 wagging, C-O stretching of substituted aromatic unit
1061	1067	C-O stretching
893	893	C-O-C stretching

Scanning Electron Microscopy (SEM)

SEM is widely utilized in adsorption studies to investigate the surface morphology of adsorbents and this allowed for the detection of any morphological changes induced by the adsorption. The SEM micrographs of Kapok husks before and after adsorption of BB3 are shown in Figure 10 (a) and (b), respectively.

As shown in Figure 10 (a), the surface appeared uneven with elongated and intertwined fibers, which are believed to be the characteristic of lignocellulosic-based materials. The materials are generally considered non-porous due to the absence of well-defined pores. After the adsorption of BB3, the surface of the Kapok husks exhibited increase roughness and notable morphological irregularities. These changes may be attributed to the attachment and agglomeration of BB3 dye molecules onto the husk surface. Such observation further confirmed the effectiveness of Kapok husks in adsorbing BB3 from solution.

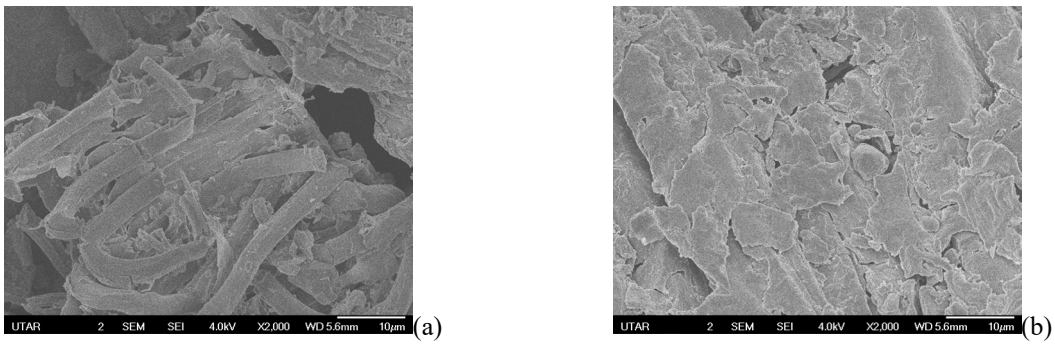

Figure 10: SEM micrographs of Kapok husks before (a) and after (b) adsorption of BB3

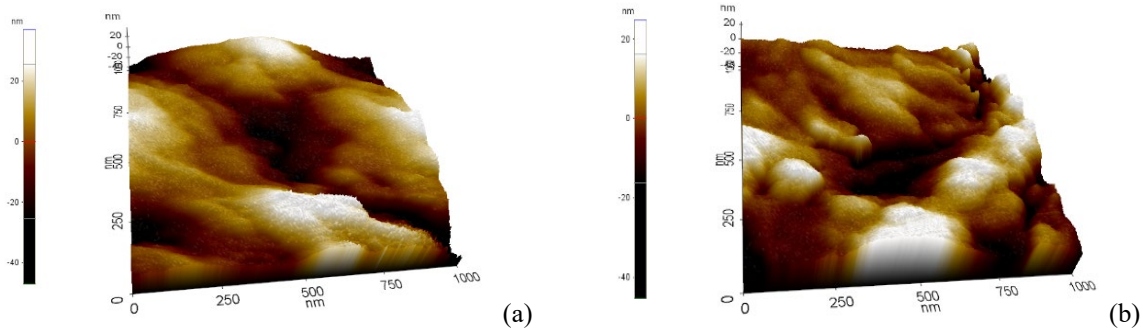

Figure 11: AFM micrographs of Kapok husks before (a) and after (b) adsorption of BB3

Atomic Force Microscopy (AFM)

In this study, the surface topography of Kapok husks was analyzed using non-contact mode AFM over a 1 × 1 μm² area. Figure 11 (a) and (b) display topographical images of the Kapok husks before and after the adsorption of BB3, respectively. The images were represented through color mapping, where darker regions indicate lower topography and lighter regions denote higher topography.[53]

Before the adsorption, the AFM image of Kapok husks showed a granular appearance and a greater presence of dark regions. This suggested the existence of a deep dent region on the surface of Kapok husks. Following the adsorption process, it was evident that the surface roughness of Kapok husks was significantly reduced, resulting in a noticeably smoother surface. Besides, the AFM image appeared overall lighter in colour after the adsorption of BB3. During the removal process, the adsorption of dye molecules onto the surface of Kapok husks led to a more pronounced surface texture, which accounts for the increased topography observed after the process.

Optimization studies

Plackett-Burman (PB) design

The Plackett-Burman design has proven to be a highly efficient method for screening and identifying key factors influencing dye adsorption.[28] Several experimental trials were carried out under different conditions as suggested by the PB. The ANOVA results for the adsorption system are presented in Table 4.

A *p*-value less than 0.05 indicated statistical significance, meaning the corresponding factor likely has a strong influence on the model's response. As shown in the table, four out of five variables, *i.e.* contact time, initial BB3 concentration, adsorbent dosage and pH, were identified as significant factors, while agitation rate was found to be insignificant in affecting the adsorption of BB3 by Kapok husks. The batch study results further supported the significance of these four factors. Subsequently, central composite design (CCD) under the Response Surface Methodology (RSM) framework was used to determine the optimum levels of each factor.

Table 4
Regression analysis (ANOVA) of Plackett-Burman for the removal of BB3

Source	Sum of squares	Degree of freedom	Mean Square	F Value	*p*-value Prob > F
Model	9898.22	5	1979.64	18.53	0.0014
A - Contact time	981.36	1	981.36	9.19	0.0231
B - Initial BB3 concentration	956.62	1	956.62	8.96	0.0242
C - Adsorbent dosage	5211.01	1	5211.01	48.79	0.0004
D - Agitation rate	35.18	1	35.18	0.33	0.5869
E - pH	2714.05	1	2714.05	25.41	0.0024
Residual	640.89	6	106.82		
R-Squared	0.9392	C.V.%		17.21	
Adjusted R-Squared	0.8885	Adequate precision		12.29	
Predicted R-Squared	0.7568				

Table 5
Experimental conditions of PB for adsorption of BB3 using Kapok husks, with both experimental and predicted uptake

Experimental run	Factors					Experimental % uptake	Predicted % uptake
	Contact time (min)	Initial BB3 concentration (mg/L)	Adsorbent dosage (g)	Agitation rate (rpm)	pH		
1	1	50	0.005	50	2	20.31	25.78
2	1	50	0.005	200	2	21.57	22.36
3	1	50	0.030	50	10	94.00	97.54
4	1	150	0.005	200	10	40.24	34.58
5	1	150	0.030	200	2	46.66	46.18
6	1	150	0.030	50	10	83.33	79.68
7	180	50	0.005	50	10	85.64	73.95
8	180	50	0.030	200	2	94.24	82.12
9	180	50	0.030	200	10	98.18	93.22
10	180	150	0.005	50	2	18.37	26.01
11	180	150	0.005	200	10	49.21	52.67
12	180	150	0.030	50	2	68.99	67.69

Verification of Plackett-Burman design model

To validate the model, the desirability function was applied. Experiments were conducted based on the optimal conditions suggested by the software. The outcomes showed strong alignment between the predicted values and the actual experimental results (Table 5).

Response Surface Methodology (RSM)

RSM involves a collection of mathematical and statistical techniques used to analyse the effects of multiple independent variables.[54] It helps in developing an accurate mathematical model of the process and provides insights into how different variables interact with one another. In this study, the significant factors identified through PB were then further examined using RSM to evaluate their influence on BB3 dye removal by Kapok husks. A total of thirty sets of experiments were generated by the system with varying conditions and the corresponding ANOVA table, derived from the experimental data is shown in Table 6. The following equation was the modified cubic models that illustrated the relationship between the four significant factors and the percentage uptake of BB3 dye:

$$\text{Uptake removal (\%)} = 1.51832 + 0.28998*A - 0.5095*B + 5396.87537*C + 11.52284*D - 0.000459427*AB + 1.88448*AC - 0.011377*AD + 2.25259*BC + 0.015557*BD - 117.01263*CD - 0.000826159*A^2 + 0.00141636*B^2 - 96595.18169*C^2 - 0.54135*D^2 \quad (14)$$

where A = contact time, B = initial BB3 concentration, C = adsorbent dosage, D = pH.

Based on the ANOVA table, the model was proven to be significant as the *p*-value of the model shown was less than 0.0001. The model F-value of 40.86 also indicated that the model is statistically significant, with only a 0.01% probability that such a high F-value could be the result of random variation or experimental noise. Contact time, initial BB3 concentration, adsorbent dosage and pH also appeared to have a *p*-value of less than 0.05, further indicating they were significant factors. In addition to this, the R^2 value was reported as 0.9744, implying that 97.44% of the variability in the response could be explained by the independent variables, while the remaining 2.56% was attributed to residue. This relatively high R^2 value, which is close to unity, reflected a strong agreement between the experimental and predicted results. The R^2 value was also in a reasonable agreement with the adjusted R^2 and predicted R^2 value, which were 0.9506 and 0.8414, respectively. The model also demonstrated high reliability and precision, as evidenced by the low coefficient of variation (C.V.) of 7.49%. Besides, the adequate precision value of 23.48 suggested a strong signal, confirming that the model is suitable for exploring and optimizing the design space.

Figure 12 (a) shows the 3D surface plot that illustrates the interaction between contact time and initial BB3 concentration towards the removal of BB3. The plot shows that the best uptake of BB3 was achieved at longer contact time and lower initial BB3 concentration. At any fixed initial concentration, the uptake steadily increased as contact time lengthens, eventually plateauing. This indicated that extended exposure allowed more dye

molecules to interact with and bind to the available active sites on the adsorbent surface. In contrast, higher initial dye concentrations resulted in reduced removal efficiency even at long contact times, since more dye molecules compete for the same finite number of sites. Changes in initial dye concentration cause greater variability in the system's response as the *p* value reported for initial BB3 concentration was 0.0002, which was less than contact time of having *p* value of 0.0013. This explained why the changes in initial dye concentration have a more pronounced effect on uptake than extending the contact time. The system likely reached adsorption equilibrium before 180 minutes, so extending the contact time beyond that point had minimal impact on further dye uptake.

Figure 12 (b) shows the 3D surface plot for the correlation between contact time and adsorbent dosage on the uptake removal of BB3. The highest dye uptake was achieved at longer contact times and with a higher amount of adsorbent. However, similarly once equilibrium was reached, further increase in contact time led to only minor improvements in removal efficiency. On the other hand, increasing the adsorbent dosage enhanced BB3 uptake due to the greater surface area and the higher number of available binding sites for dye adsorption.

Table 6
Regression analysis (ANOVA) of RSM for the removal of BB3

Source	Sum of squares	Degree of freedom	Mean square	F Value	*p*-value Prob > F
Model	18686.62	14	1334.76	40.86	< 0.0001
A-Contact time	505.65	1	505.65	15.48	0.0013
B-Initial BB3 concentration	820.72	1	820.72	25.12	0.0002
C-Adsorbent dosage	8221.84	1	8221.84	251.69	< 0.0001
D-pH	3538.01	1	3538.01	108.31	< 0.0001
AB	67.63	1	67.63	2.07	0.1707
AC	71.12	1	71.12	2.18	0.1608
AD	265.42	1	265.42	8.13	0.0122
BC	31.71	1	31.71	0.97	0.3401
BD	154.89	1	154.89	4.74	0.0458
CD	547.68	1	547.68	16.77	0.0010
A^2	113.47	1	113.47	3.47	0.0821
B^2	32.48	1	32.48	0.99	0.3345
C^2	590.21	1	590.21	18.07	0.0007
D^2	194.38	1	194.38	5.96	0.0276
Residual	490.00	15	32.67		
Lack of fit	490.00	10	49.00		
R-Squared	0.9744		C.V.%		7.49
Adjusted R-Squared	0.9506		Adequate Precision		23.48
Predicted R-Squared	0.8414				

The relationship between contact time, pH and uptake removal of BB3 is illustrated in Figure 12 (c). The trend of percentage uptake over contact time closely resembles the one shown in Figure 12 (b), whereas higher pH conditions were found to enhance BB3 adsorption, with uptake increasing as pH increased and stabilizing beyond pH 6. This was likely due to the electrostatic attraction between the positively charged BB3 dye and the negatively charged surface of the Kapok husks, resulting in a high removal efficiency.

Figure 12 (d) shows that high removal efficiency could be achieved when the adsorption system was subjected to low initial BB3 concentration and high adsorbent dosage. The effect of adsorbent dosage was similar, as previously discussed. Similarly, at low initial dye concentrations, fewer molecules compete for binding sites, leading to higher removal efficiency. Figure 12 (e) and (f) presents the 3D surface plots showing the correlation between pH and initial BB3 concentration, and between pH and adsorbent dosage, respectively, in relation to uptake removal. The trend of the effect of initial BB3 concentration on uptake removal was as discussed previously, whereas the uptake pattern against pH resembled that in Figure 12 (c), where it plateaued beyond pH 6. The percentage uptake increased with increasing

adsorbent dosage, following a similar trend seen in Figure 12 (b).

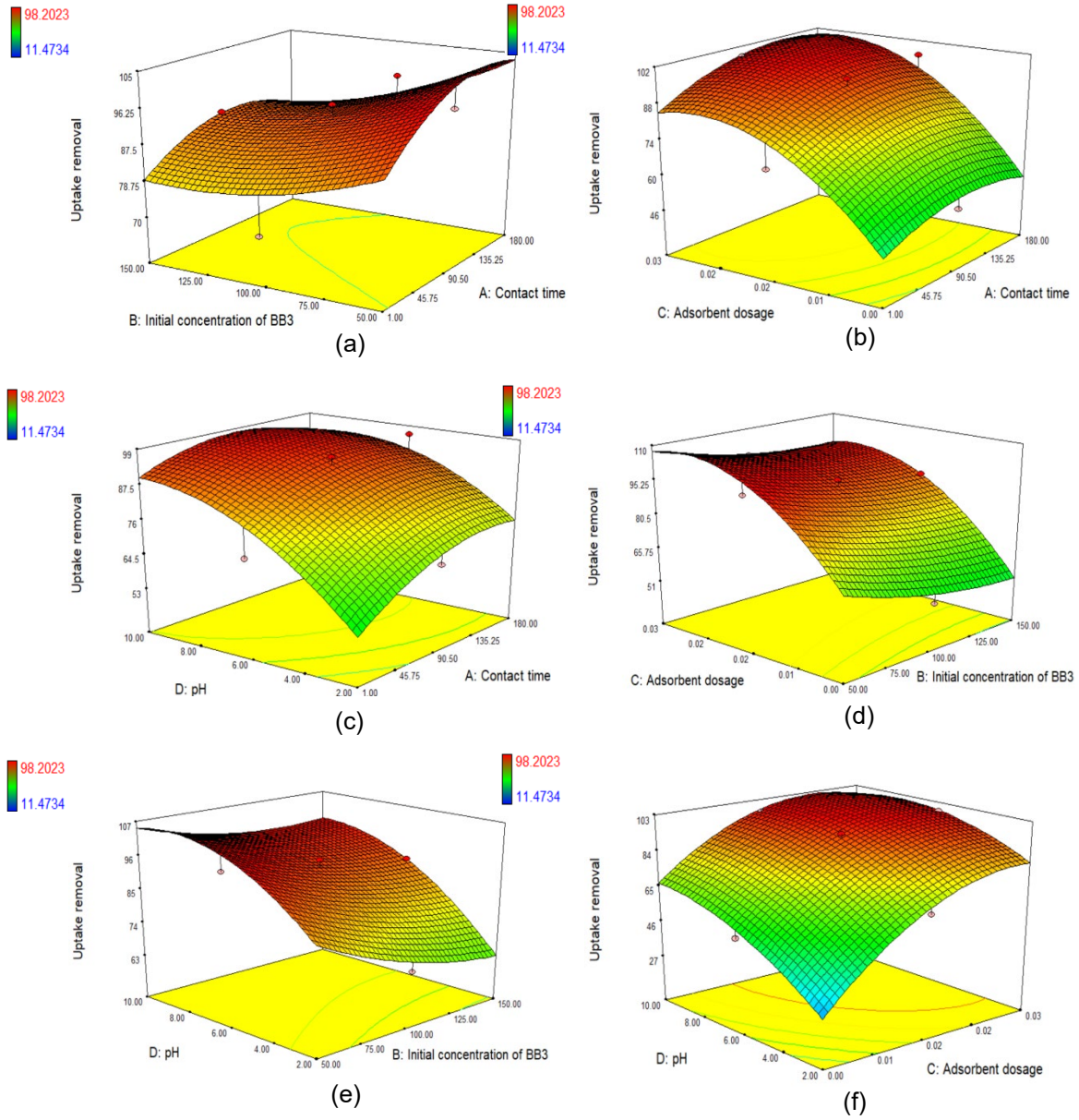

Figure 12: 3D surface plot for the removal of BB3 using Kapok husks as a function of (a) contact time and initial BB3 concentration, (b) contact time and adsorbent dosage, (c) contact time and pH, (d) initial BB3 concentration and adsorbent dosage, (e) initial BB3 concentration and pH, (f) adsorbent dosage and pH

Verification of RSM models

The proposed model equation was validated using the desirability function under optimum conditions suggested by the software. As shown in Table 7, the predicted and experimental uptake values of BB3 dye were closely aligned, with percentage discrepancies all below 10%. This small variation confirmed the reliability and validity of the model.

Table 7
Experimental conditions of RSM for adsorption of BB3 using Kapok husks, with both experimental and predicted uptake.

Experimental run	Factors				Experimental % uptake	Predicted % uptake
	Contact time (min)	Initial BB3 concentration (mg/L)	Adsorbent dosage (g)	pH		
1	1	50	0.005	2	24.80	26.24
2	1	50	0.005	10	65.75	67.90
3	1	50	0.03	2	80.41	73.65
4	1	50	0.03	10	95.10	91.91
5	1	100	0.0175	6	70.39	80.44
6	1	150	0.005	2	11.47	19.60
7	1	150	0.005	10	67.74	61.91
8	1	150	0.03	2	57.29	60.85
9	1	150	0.03	10	89.35	91.56
10	90.5	50	0.0175	6	97.57	87.59
11	90.5	100	0.0175	2	66.38	69.68
12	90.5	100	0.0175	6	94.85	92.36
13	90.5	100	0.005	6	51.62	55.89
14	90.5	100	0.0175	10	96.03	97.72
15	90.5	100	0.03	6	97.93	96.19
16	90.5	150	0.0175	6	89.25	89.15
17	180	50	0.005	2	46.26	44.88
18	180	50	0.005	10	75.88	70.25
19	180	50	0.03	2	96.96	98.12
20	180	50	0.03	10	98.20	97.08
21	180	100	0.0175	6	96.11	91.04
22	180	150	0.005	2	17.14	18.22
23	180	150	0.005	10	48.46	56.04
24	180	150	0.03	2	81.02	79.70
25	180	150	0.03	10	97.62	94.11

CONCLUSION

In this current work, Kapok husks were proven to be an effective and potential adsorbent for the removal of BB3 from aqueous solution. The equilibrium adsorption data was determined to be well-suited to both Langmuir and BET isotherm models compared to the Freundlich isotherm model. The maximum adsorption capacity of 197.1 mg/g with an R^2 value of 0.9972 were obtained. The adsorption system was found to obey the pseudo-second order kinetic model with R^2 close to unity. Plackett-Burman design identified contact time, initial BB3 concentration, adsorbent dosage and pH as the significant factors in the adsorption of BB3 by Kapok husks. The optimum conditions for maximum BB3 adsorption were determined using RSM, with a model equation developed and 3D surface plots illustrating the interactions between BB3 uptake and significant factors. A maximum BB3 removal efficiency of 98.20% was achieved under optimum conditions of 180 minutes contact time, 50 mg/L of initial BB3 concentration, 0.03 g of Kapok husks and pH 10.

ACKNOWLEDGMENTS: This research work received financial support and research facilities assistance from Universiti Tunku Abdul Rahman.

REFERENCES

[1] R. Jamee and R. Siddique, *Eur. J. Microbiol. Immunol.*, **9**, 114 (2019), https://doi.org/10.1556/1886.2019.00018
[2] S. Pourrahim, A. Salem, S. Salem and R. Tavangar, *Environ. Pollut.*, **256**, 113454 (2020), https://doi.org/10.1016/j.envpol.2019.113454
[3] A. R. Gregory, S. Elliot and P. Kludge, *J. Appl. Toxicol.*, **1**, 308 (1991)
[4] K. Hunger, "Industrial Dyes: Chemistry, Properties, Applications", Wiley-VCH, Weinheim, 2003
[5] M. Felista Mutunga, W. C. Wanyonyi and G. Ongera, *Environ. Chem. Ecotoxicol.*, **2**, 194 (2020), https://doi.org/10.1016/j.enceco.2020.09.005
[6] T. Wang, L. Han, X. Li, T. Chen and S. Wang, *Front. Chem.*, **10**, 962383 (2022), https://doi.org/10.3389/fchem.2022.962383
[7] B. Morali and T. B. Budak, *Molecules*, **30**, 4039 (2025), https://doi.org/10.3390/molecules30204039

[8] K. Rupali, T. Patil and M. Dipak, *Int. J. Fish. Aquat. Stud.*, **12**, 26 (2024), https://doi.org/10.22271/fish.2024.v12.i1a.2887
[9] P. S. Kumar, G. J. Joshiba, C. C. Femina, P. Varshini, S. Priyadharshini *et al.*, *Desalin. Water Treat.*, **172**, 395 (2019), https://doi.org/10.5004/dwt.2019.24613
[10] D. A. Gkika, A. K. Tolkou, I. A. Katsoyiannis and G. Z. Kyzas, *Sep. Purif. Technol.*, **368**, 132996 (2025), https://doi.org/10.1016/j.seppur.2025.132996
[11] A. Mariyam, J. Mittal, F. Sakina, R. T. Baker, A. K. Sharma *et al.*, *Arab. J. Chem.*, **14**, 103186 (2021), https://doi.org/10.1016/j.arabjc.2021.103186
[12] D. Gang, Z. U. Ahmad, Q. Lian, L. Yao and M. E. Zappi, *Chem. Eng. J.*, **403**, 126286 (2021), https://doi.org/10.1016/j.cej.2020.126286
[13] J. O. Quansah, T. Hlaing, F. N. Lyonga, P. P. Kyi, S. H. Hong *et al.*, *Appl. Sci.*, **10**, 3437 (2020), https://doi.org/10.3390/app10103437
[14] S. J. Salih, A. S. A. Kareem and S. S. Anwer, *Heliyon*, **8**, e10092 (2022), https://doi.org/10.1016/j.heliyon.2022.e10092
[15] S. L. Chan, Y. P. Tan, A. H. Abdullah and S. T. Ong, *J. Taiwan Inst. Chem. Eng.*, **61**, 306 (2016), https://doi.org/10.1016/j.jtice.2016.01.010
[16] M. Akter, F. B. A. Rahman, M. Z. Abedin and S. M. F. Kabir, *Textiles*, **1**, 361 (2021), https://doi.org/10.3390/textiles1020018
[17] E. W. C. Chan, S. W. Yeong, C. W. Wong, O. Y. M. Soo, A. C. Y. Phua *et al.*, *J. Appl. Biol. Biotech.*, **11**, 1 (2023), https://dx.doi.org/10.7324/JABB.2023.110101
[18] K. C. Vasconcelos, S. G. Alencar, A. B. Ferro, L. F. A. M. Oliveira, E. J. S. Fonseca *et al.*, *Sep. Purif. Technol.*, **326**, 124787 (2023), https://doi.org/10.1016/j.seppur.2023.124787
[19] R. Zein, H. Fathony, P. Ramadhani and D. Deswati, *J. Serb. Chem. Soc.*, **89**, 123 (2024), https://doi.org/10.2298/JSC230303084Z
[20] T. J. Al-Musawi, A. H. Mahvi, A. D. Khatibi and D. Balarak, *J. Porous Mater.*, **28**, 835 (2021), https://doi.org/10.1007/s10934-021-01039-7
[21] B. A. Fil, M. Yilmaz, S. Bayar and M. T. Elkoca, *Braz. J. Chem. Eng.*, **31**, 171 (2014), https://doi.org/10.1590/S0104-66322014000100016
[22] G. D. Değermenci, N. Değermenci, V. Ayvaoğlu, E. Durmaz, D. Çakır *et al.*, *J. Clean. Prod.*, **225**, 1220 (2019), https://doi.org/10.1016/j.jclepro.2019.03.260
[23] H. Shayesteha, A. Rahbar-Kelishamia and R. Norouzbeigia, *Desalin. Water Treat.*, **57**, 12822 (2016), https://doi.org/10.1080/19443994.2015.1054315
[24] M. K. Obaid, L. C. Abdullah and I. J. Idan, *J. Chem.*, **4262578** (2016), https://doi.org/10.1155/2016/4262578
[25] W. Y. Chung and S. T. Ong, *J. Phys. Sci.*, **32**, 91 (2021), https://jps.usm.my/wp-content/uploads/2021/04/JPS-321_Art.-7_91-108-1.pdf
[26] G. K. Latinwo, A. O. Alade, S. E. Agarry and E. O. Dada, *Polycycl. Aromat. Comp.*, **41**, 400 (2019), https://doi.org/10.1080/10406638.2019.1591467
[27] K. Kuśmierek and A. Świątkowski, *React. Kinet. Mech. Catal.*, **116**, 261 (2015), https://doi.org/10.1007/s11144-015-0889-1
[28] K. T. Chan, S. T. Ong and S. T. Ha, *Cellulose Chem. Technol.*, **59**, 207 (2025), https://doi.org/10.35812/CelluloseChemTechnol.2025.59.19
[29] J. K. Chong and S. T. Ong, *Stud. Univ. Babes-Bolyai Chem.*, **66**, 171 (2021), https://chem.ubbcluj.ro/~studiachemia/chemia2021_4.html#download13
[30] I. Langmuir, *J. Am. Chem. Soc.*, **40**, 1361 (1918)
[31] Z. Bencheqroun, I. E. Mrabet, M. Nawdali, M. Benali and H. Zaitan, *Desalin. Water Treat.*, **240**, 177 (2021), https://doi.org/10.5004/dwt.2021.27635
[32] M. Sadia, I. Ahmad, F. Ali, M. Zahoor, R. Ullah *et al.*, *Molecules*, **27**, 3276 (2022), https://doi.org/10.3390/molecules27103276
[33] H. M. F. Freundlich, *J. Phys. Chem.*, **57**, 385 (1906)
[34] S. Brunauer, P. H. Emmett and E. Teller, *J. Am. Chem. Soc.*, **60**, 309 (1938)
[35] S. Lagergren, *Kungl. Svenska Vetenskapsakad. Handl.*, **24**, 1 (1898)
[36] Y. S. Ho and G. McKay, *Process Biochem.*, **34**, 451 (1999), https://doi.org/10.1016/S0032-9592(98)00112-5
[37] H. Alyasi, H. Mackey and G. McKay, *Molecules*, **28**, 6561 (2023), https://doi.org/10.3390/molecules28186561
[38] M. Foroughi-Dahr, H. Abolghasemi, M. Esmaili, A. Shojamoradi and H. Fatoorehchi, *Chem. Eng. Commun.*, **202**, 181 (2015), https://doi.org/10.1080/00986445.2013.836633
[39] V. Essel and D. E. Raynie, *Separations*, **12**, 37 (2025), https://doi.org/10.3390/separations12020037
[40] Y. Chang, R. An, S. Sun, M. Hou, F. Han *et al.*, *Molecules*, **29**, 2619 (2024), https://doi.org/10.3390/molecules29112619
[41] J. Shi and J. Li, *BioResources*, **7**, 3463 (2012), https://bioresources.cnr.ncsu.edu/wp-content/uploads/2016/06/BioRes_07_3_3463_Shi_Li_Metabolites_Chem_Group_Pine_Inclining_2408.pdf
[42] J. Zhuang, M. Li, Y. Pu, A. Ragauskas and C. Yoo, *Appl. Sci.*, **10**, 4345 (2020), https://doi.org/10.3390/app10124345
[43] H. Bian, Y. Yang and P. Tu, *BioResources*, **16**, 8353 (2021), https://bioresources.cnr.ncsu.edu/wp-content/uploads/2021/10/BioRes_16_4_8353_Bian_YT_Crystal_Struc_All_Cellulose_Nanocomposites_Corn_Wheat_Straw_19127.pdf
[44] F. Fink, F. Emmerling and J. Falkenhagen, *Chem. Meth.*, **1**, 354 (2021), https://doi.org/10.1002/cmtd.202100028
[45] D. L. Sills and J. M. Gossett, *Biotechnol. Bioeng.*, **109**, 353 (2011), https://doi.org/10.1002/bit.23314
[46] Z. Li, H. Hanafy, L. Zhang, L. Sellaoui, M. S. Netto *et al.*, *Chem. Eng. J.*, **388**, 124263 (2020), https://doi.org/10.1016/j.cej.2020.124263

[47] S. Srivastava and G. Mathur, *The Microbe*, **7**, 100340 (2025), https://doi.org/10.1016/j.microb.2025.100340
[48] H. Y. Gan, L. E. Leow and S. T. Ong, *Acta Chim. Slov.*, **64**, 144 (2017), https://doi.org/10.17344/acsi.2016.2983
[49] S. L. Lee, S. W. Liew and S. T. Ong, *Acta Chim. Slov.*, **63**, 144 (2016), https://doi.org/10.17344/acsi.2015.2068
[50] A. Yildirim, *Chem. Eng. Technol.*, **44**, 1371 (2021), https://doi.org/10.1002/ceat.202100077
[51] A. Tarik, F. Khammour, M. Talbi and M. Kouali, *Orient. J. Chem.*, **30**, 1183 (2014), https://dx.doi.org/10.13005/ojc/300332
[52] M. Roulia and A. A. Vassiliadis, *Agronomy*, **11**, 1625 (2021), https://doi.org/10.3390/agronomy11081625
[53] S. T. Ong and W. N. Lee, *Desalin. Water Treat.*, **57**, 18157 (2015), https://doi.org/10.1080/19443994.2015.1088474
[54] R. H. Myers and D. C. Montgomery, "Response Surface Methodology – Process and Product Optimization Using Designed Experiments", 2nd ed., John Wiley & Sons, New York, 2002